Generalized QCTO for Metamaterial-Lens-Coated Conformal Arrays

Giacomo Oliveri, *Senior Member, IEEE*, Ephrem T. Bekele, Douglas H. Werner, *Fellow, IEEE*, Jeremiah P. Turpin, *Member, IEEE*, and Andrea Massa, *Member, IEEE*

***Abstract*—The use of inhomogeneous metamaterial lenses is proposed to enable suitable radiation properties for arbitrary-shape antenna arrays. Towards this end, the Quasi-Conformal Transformation Optics (QCTO) methodology is generalized to allow an *arbitrary* physical arrangement coated with a suitable lens to exhibit the same radiating features of an *arbitrary* reference virtual array in free space. A representative numerical example, concerned with a two-dimensional layout, is presented to assess the effectiveness of the proposed method as well as the enhanced features of the resulting metamaterial-coated arrays with respect to standard conformal arrangements.**

***Index Terms*—Circular arrays, conformal arrays, dielectric lenses, material-by-design, metamaterials, quasi-conformal transformation optics (QCTO).**

I. Introduction and Motivation

CONTROLLING the beam shape and the radiation features during scanning is fundamental in phased array applications, such as radar [1], remote sensing [2], and communication systems [3], [4], where the resolution, the sensitivity, or the gain of the antenna must be invariant in azimuth and/or elevation. This is the main motivation behind the success of circular arrangements in phased array design since they intrinsically avoid beam distortions owing to their radial symmetry [1]–[4]. Unfortunately, circular layouts cannot be employed whenever the antenna shape is heavily constrained by mechanical/aerodynamic requirements [5] as in satellites and aircrafts. Therefore, it is of great interest from the scientific and industrial viewpoint to design arbitrary-shaped (i.e., conformal) arrangements that exhibit a steering-controlled beam shape (as in circular arrays) or, more in general, that fit user-defined reference beam-shape requirements. In such a framework, the use of lenses of artificial inhomogeneous (and possibly anisotropic) materials turns out to be a promising solution to adapt and customize the radiating features of arbitrary antenna arrays (e.g., beam shape versus steering angle) to meet specific application/user requirements [6], [7]. Indeed, the exploitation of inhomogeneous media engineered through suitable *Material-by-Design* strategies [8], [9] has recently been used for electromagnetic field manipulations to synthesize invisibility cloaks, field-rotating devices, field concentrators, and polarization splitters (see [10]–[14] and the references therein).

Towards this end, *Quasi-Conformal Transformation Optics* (QCTO) has been introduced as a powerful theory to design non- magnetic broadband $2D$ lenses capable of modifying the field propagation according to the user-defined needs and requirements [7]. It is based on the form-invariance of Maxwell's equations under a suitable coordinate transformation [7], [15]. Its key advantage over other Transformation Optics (TO) techniques [11] relies on the fact that the coordinate transformation is enforced to be "smooth" so that the final lens layout usually exhibits a reduced anisotropy and non-magnetic properties [7]. More specifically, the QCTO establishes a mapping between [7], [15]

- a starting "*virtual*" geometry, which is characterized by known permittivity and permeability profiles and it presents the desired radiation features without regard to fitting the shape constraints,

and

- a final "*physical*" layout, satisfying the shape constraints, whose permittivity and permeability have to be determined so that the radiated field exactly reproduces that of the virtual geometry.

From an algorithmic viewpoint, the QCTO inputs are the virtual geometry and the lens shape (also indicated as "physical" geometry) plus the electromagnetic parameters (i.e., the dielectric features and the electromagnetic sources) of the *virtual* layout, while the corresponding outputs are the permittivity and the permeability profiles of the *final* lens layout. Based on these unique features, QCTO has been recently exploited to synthesize radiating structures affording controlled beam scanning [7]. In that case, the virtual geometry was a circular antenna arrangement surrounded by a "free space box", while the physical layout was a linear array coated with a suitable QCTO lens [7]. Despite the interesting results, the QCTO synthesis scheme proposed in [7] turns out to be limited to linear-to-conformal (or *vice-versa*) array transformations, while it cannot be directly applied to transformation electromagnetic problems where both virtual and physical layouts have arbitrary shapes.

This work is then aimed at extending the QCTO technique proposed in [7] to the design of conformal arrays matching the radiation properties of an arbitrarily user-defined virtual array. Towards this end, the QCTO method is generalized by means of

Manuscript received November 17, 2013; revised March 28, 2014; accepted May 10, 2014. Date of publication June 02, 2014; date of current version July 31, 2014. This work was supported in part by the EMERALD Project funded by the Autonomous Province of Trento, Calls for Proposal "Team 2011".

G. Oliveri, E. T. Bekele, and A. Massa are with the ELEDIA Research Center@DISI, University of Trento, 38123 Trento, Italy (e-mail: andrea.massa@unitn.it; giacomo.oliveri@disi.unitn.it; ephrem.bekele@disi.unitn.it).

J. P. Turpin and D. H. Werner are with Pennsylvania State University, University Park, PA 16801 USA and also with the EMERALD Research Unit, University of Trento, Trento, Italy (e-mail: dhw@psu.edu; jpt189@psu.edu).

Color versions of one or more of the figures in this paper are available online at http://ieeexplore.ieee.org.

Digital Object Identifier 10.1109/TAP.2014.2327643

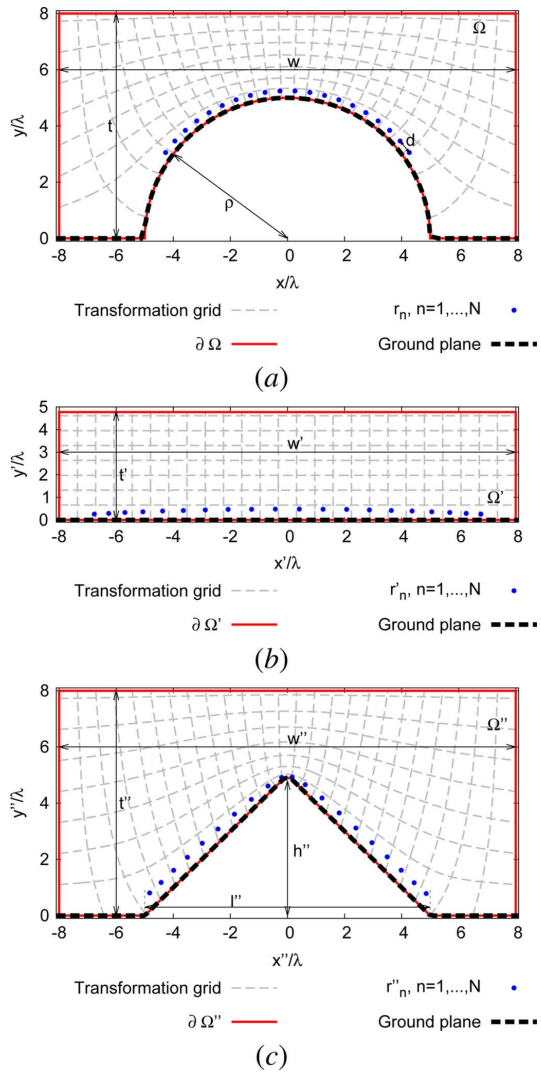

Fig. 1. [*Problem Geometry*] Coordinate system and transformation grids for $2D$ conformal array over a ground plane: (*a*) *virtual* geometry, (*b*) *intermediate* geometry, and (*c*) *physical* geometry.

a two-step transformation strategy enabling the definition of arbitrary *virtual* and *physical* layouts. Such a strategy is motivated by the fact that it enables to decompose the overall transformation into two concatenated QCTO steps that require the solution of two standard Laplace equations, that is (*i*) the transformation of an arbitrary virtual geometry into a rectangular *intermediate* one, and (*ii*) the transformation of this latter into the arbitrary physical one. A set of representative full-wave numerical results, concerned with edge-shaped arrays with steering-controlled beams in the $2D$ transverse-magnetic (TM) case, are then presented to assess the effectiveness and the flexibility of the proposed approach.

II. Problem Formulation and QCTO Solution

With reference to a time-harmonic[1] generic TO problem [7], [11], let us consider the *virtual* scenario represented by an arbitrary-shaped domain of extension Ω characterized by permittivity and permeability tensors defined as $\bar{\bar{\varepsilon}}(\mathbf{r})$ and $\bar{\bar{\mu}}(\mathbf{r})$, respectively, where $\mathbf{r} = (x, y, z)$ represents a point in the *virtual* coordinate system [Fig. 1(*a*)]. A *virtual* array of N antennas, which are modeled as N electric current line sources, $\mathbf{J}_n(\mathbf{r}) = J_n\delta(x - x_n, y - y_n)\hat{z}$, $n = 1, \ldots, N$ (J_n and $\mathbf{r}_n \in \Omega$ being the complex amplitude and the position of the n-th array element, respectively), is assumed to generate the electric and magnetic field distributions $\mathbf{E}(\mathbf{r})$ and $\mathbf{H}(\mathbf{r})$. Let us then consider a *physical* domain of extension Ω'' characterized by (unknown) dielectric tensors $\bar{\bar{\varepsilon}}''(\mathbf{r}'')$ and $\bar{\bar{\mu}}''(\mathbf{r}'')$, such that $\mathbf{r}'' = (x'', y'', z'')$ is the *physical* coordinate system [Fig. 1(*c*)] that results from Ω by means of a vectorial coordinate transformation

$$\mathbf{r}'' = \mathbf{\Gamma}(\mathbf{r}) \triangleq \begin{bmatrix} \Gamma_x(\mathbf{r}) \\ \Gamma_y(\mathbf{r}) \\ \Gamma_z(\mathbf{r}) \end{bmatrix}, \quad \mathbf{r} \in \Omega,\ \mathbf{r}'' \in \Omega''. \tag{1}$$

The objective of the QCTO method is to determine the N transformed antenna sources $\mathbf{J}''_n(\mathbf{r}'') = J''_n\delta(x'' - x''_n, y'' - y''_n)\hat{z}''$, $n = 1, \ldots, N$ (J''_n and $\mathbf{r}''_n \in \Omega''$ being their complex amplitudes and positions, respectively) and the transformed permittivity/permeability distributions $\bar{\bar{\varepsilon}}''(\mathbf{r}'')$ and $\bar{\bar{\mu}}''(\mathbf{r}'')$ that generate outside Ω'' the *physical* distributions, $\mathbf{E}''(\mathbf{r}'')$ and $\mathbf{H}''(\mathbf{r}'')$, equal to those of the *virtual* problem, $\mathbf{E}(\mathbf{r})$ and $\mathbf{H}(\mathbf{r})$, outside Ω. In other words,

$$\begin{cases} \mathbf{E}''(\mathbf{r}'') \approx \mathbf{E}(\mathbf{r}) \\ \mathbf{H}''(\mathbf{r}'') \approx \mathbf{H}(\mathbf{r}) \end{cases} \quad \text{if } \mathbf{r} = \mathbf{r}'', \mathbf{r} \notin \Omega, \mathbf{r}'' \notin \Omega''. \tag{2}$$

The key step for solving such a problem is the computation of the so-called *deformation field* $\mathbf{\Gamma}(\mathbf{r})$ in (1) [16]. This is generally very complicated because of the difficulties in analytically expressing the shape of arbitrary Ω and Ω'' contours [16]. Moreover, $\mathbf{\Gamma}(\mathbf{r})$ must be as smooth as possible [otherwise, physically unfeasible $\bar{\bar{\varepsilon}}''(\mathbf{r}'')$ and $\bar{\bar{\mu}}''(\mathbf{r}'')$ arise] [7], [15]–[17]. Such a requirement has suggested $\mathbf{\Gamma}(\mathbf{r})$ be defined such that it complies with a Laplace's equation subject to Dirichlet boundary conditions since it always gives rise to harmonic (i.e., smooth) solutions [15], [16]. More specifically, the QCTO approach numerically determines $\mathbf{\Gamma}(\mathbf{r})$ by solving the following Laplace equation [15], [16]

$$\begin{cases} \nabla^2[\mathbf{\Gamma}(\mathbf{r})] = 0 \quad \mathbf{r} \in \Omega \\ \mathbf{\Gamma}(\mathbf{r})|_{\mathbf{r}=\partial\Omega} = \partial[\Omega''] \end{cases} \tag{3}$$

where $\partial\Omega$ and $\partial[\Omega'']$ are the contours of the *virtual* [Fig. 1(*a*)] and the *physical* domains [Fig. 1(*c*)].

However, the computation of (3) by state-of-the-art QCTO techniques requires that either Ω or Ω'' are "regular" (i.e., one of the domains has a rectangular shape) [7], [15] so that the corresponding boundary conditions are easily expressed [15]. In fact, although the standard Laplace equation (3) could be theoretically applied when both $\partial\Omega$ and $\partial[\Omega'']$ are arbitrary, the resulting $\mathbf{\Gamma}(\mathbf{r})|_{\mathbf{r}=\partial\Omega} = \partial[\Omega'']$ condition would not be analytically expressible and implementable in this case [15]. Consequently, the exploitation of the approach in [7], [15] is not convenient for the case at hand since either one or both Ω and Ω'' can have an irregular shape.

Such a synthesis problem is then solved by exploiting a new two-step procedure based on the introduction of an *intermediate* transformation [Fig. 1(*b*)]. More specifically, the intermediate step is concerned with a rectangular domain Ω' characterized by (unknown) dielectric tensors $\bar{\bar{\varepsilon}}'(\mathbf{r}')$ and $\bar{\bar{\mu}}'(\mathbf{r}')$ [$\mathbf{r}' = (x', y', z')$

[1]The time dependency factor $\exp(j2\pi ft)$ is assumed and omitted in the following.

being the *intermediate* coordinate system—Fig. 1(*b*)] and illuminated by N current sources, $\mathbf{J}'_n(\mathbf{r}') = J'_n\delta(x'-x'_n, y'-y'_n)\hat{z}'$, located at the positions $\mathbf{r}'_n \in \Omega'$, $n = 1, \ldots, N$ with complex amplitudes J'_n that radiate the electric and magnetic field *intermediate* distributions $\mathbf{E}'(\mathbf{r}')$ and $\mathbf{H}'(\mathbf{r}')$.

The overall synthesis approach can then be summarized as follows:

1) Compute the *quasi*-conformal mapping $\mathbf{r}' = \mathbf{\Phi}(\mathbf{r}) \triangleq [\Phi_x(\mathbf{r}), \Phi_y(\mathbf{r}), \Phi_z(\mathbf{r})]$ ($\mathbf{r} \in \Omega, \mathbf{r}' \in \Omega'$), then derive $\bar{\bar{\varepsilon}}'(\mathbf{r}')$, $\bar{\bar{\mu}}'(\mathbf{r}')$, and $\mathbf{J}'_n(\mathbf{r})$, $n = 1, \ldots, N$, such that

$$\begin{cases} \mathbf{E}'(\mathbf{r}') \approx \mathbf{E}(\mathbf{r}) \\ \mathbf{H}'(\mathbf{r}') \approx \mathbf{H}(\mathbf{r}) \end{cases} \quad \text{if } \mathbf{r} = \mathbf{r}', \mathbf{r} \notin \Omega, \mathbf{r}' \notin \Omega'. \tag{4}$$

2) Compute the *quasi*-conformal mapping $\mathbf{r}'' = \mathbf{\Psi}(\mathbf{r}') \triangleq [\Psi_{x'}(\mathbf{r}'), \Psi_{y'}(\mathbf{r}'), \Psi_{z'}(\mathbf{r}')]$ ($\mathbf{r}' \in \Omega', \mathbf{r}'' \in \Omega''$), then derive $\bar{\bar{\varepsilon}}''(\mathbf{r}'')$, $\bar{\bar{\mu}}''(\mathbf{r}'')$, and $\mathbf{J}''_n(\mathbf{r})$, $n = 1, \ldots, N$, such that

$$\begin{cases} \mathbf{E}''(\mathbf{r}'') \approx \mathbf{E}'(\mathbf{r}') \\ \mathbf{H}''(\mathbf{r}'') \approx \mathbf{H}'(\mathbf{r}') \end{cases} \quad \text{if } \mathbf{r}' = \mathbf{r}'', \mathbf{r}' \notin \Omega', \mathbf{r}'' \notin \Omega''. \tag{5}$$

Since Ω' is rectangular, the two above sub-problems fall within the QCTO assumptions [7], [15], [16]. Accordingly, the deformation fields $\Phi(\mathbf{r})$ and $\Psi(\mathbf{r}')$ can be determined by numerically solving the following Laplace's equations [7], [15], [16]

$$\begin{cases} \nabla^2[\mathbf{\Phi}(\mathbf{r})] = 0 \quad \mathbf{r} \in \Omega \\ \mathbf{\Phi}(\mathbf{r})|_{\mathbf{r}=\partial\Omega} = \partial[\Omega'] \end{cases} \tag{6}$$

and

$$\begin{cases} \nabla^2[\mathbf{\Psi}(\mathbf{r}')] = 0 \quad \mathbf{r}' \in \Omega' \\ \mathbf{\Psi}(\mathbf{r}')|_{\mathbf{r}'=\partial\Omega'} = \partial[\Omega''] \end{cases} \tag{7}$$

by means of state-of-the-art methods [7], [15], [16] whose implementations are available [18]. Once $\mathbf{\Phi}(\mathbf{r})$ and $\mathbf{\Psi}(\mathbf{r}')$ have been derived, the transformation optics rules [7], [15]–[17] can be applied to yield

$$\bar{\bar{\varepsilon}}'(\mathbf{r}') = \left.\frac{\mathcal{J}[\mathbf{\Phi}(\mathbf{r})]\bar{\bar{\varepsilon}}(\mathbf{r})\mathcal{J}^T[\mathbf{\Phi}(\mathbf{r})]}{\det\{\mathcal{J}[\mathbf{\Phi}(\mathbf{r})]\}}\right|_{\mathbf{r}=\mathbf{r}'} \tag{8}$$

$$\bar{\bar{\varepsilon}}''(\mathbf{r}'') = \left.\frac{\mathcal{J}[\mathbf{\Psi}(\mathbf{r}')]\bar{\bar{\varepsilon}}'(\mathbf{r}')\mathcal{J}^T[\mathbf{\Psi}(\mathbf{r}')]}{\det\{\mathcal{J}[\mathbf{\Psi}(\mathbf{r}')]\}}\right|_{\mathbf{r}'=\mathbf{r}''} \tag{9}$$

where $\cdot^T$ is the transpose operator, $\det\{\cdot\}$ is the determinant, and $\mathcal{J}[\mathbf{\Phi}(\mathbf{r})]$ (and $\mathcal{J}[\mathbf{\Psi}(\mathbf{r}')]$) is the Jacobian transformation tensor, defined as

$$\mathcal{J}[\mathbf{\Phi}(\mathbf{r})] = \begin{bmatrix} \frac{\partial\Phi_x(\mathbf{r})}{\partial x} & \frac{\partial\Phi_x(\mathbf{r})}{\partial y} & \frac{\partial\Phi_x(\mathbf{r})}{\partial z} \\ \frac{\partial\Phi_y(\mathbf{r})}{\partial x} & \frac{\partial\Phi_y(\mathbf{r})}{\partial y} & \frac{\partial\Phi_y(\mathbf{r})}{\partial z} \\ \frac{\partial\Phi_z(\mathbf{r})}{\partial x} & \frac{\partial\Phi_z(\mathbf{r})}{\partial y} & \frac{\partial\Phi_z(\mathbf{r})}{\partial z} \end{bmatrix} \tag{10}$$

($\mathcal{J}[\mathbf{\Psi}(\mathbf{r}')]$ is computed analogously). Moreover, the formulas for the permeability are directly obtained from (8) and (9) by the symbolic substitution $\varepsilon \leftarrow \mu$ [16]. As for the sources, a simple geometrical shift is then required to take into account the applied transformation [7], [15], [16] and to yield

$$J''_n = J'_n = J_n \tag{11}$$

and

$$\mathbf{r}''_n = \mathbf{\Psi}(\mathbf{r}'_n) = \mathbf{\Psi}(\mathbf{\Phi}(\mathbf{r}_n)) \tag{12}$$

$\mathbf{r}_n \triangleq (x_n, y_n, 0)$, $\mathbf{r}'_n \triangleq (x'_n, y'_n, 0)$, $\mathbf{r}''_n \triangleq (x''_n, y''_n, 0)$ being the location of the n-th source in the Ω, Ω', and Ω'' domains, respectively.

By combining (8) and (9), the following expression is then derived

$$\bar{\bar{\varepsilon}}''(\mathbf{r}'') = \left.\frac{\mathcal{J}[\mathbf{\Psi}(\mathbf{r}')]\left\{\left.\frac{\mathcal{J}[\mathbf{\Phi}(\mathbf{r})]\bar{\bar{\varepsilon}}(\mathbf{r})\mathcal{J}^T[\mathbf{\Phi}(\mathbf{r})]}{det\{\mathcal{J}[\mathbf{\Phi}(\mathbf{r})]\}}\right|_{\mathbf{r}=\mathbf{r}'}\right\}\mathcal{J}^T[\mathbf{\Psi}(\mathbf{r}')]}{\det\{\mathcal{J}[\mathbf{\Psi}(\mathbf{r}')]\}}\right|_{\mathbf{r}'=\mathbf{r}''} \tag{13}$$

to provide, in conjunction with (11) and (12), the numerical solution to the *Material-by-Design* problem at hand.

It is worth noticing that the proposed procedure is uniquely defined once the shape and the size of Ω, Ω', and Ω'' are specified by the designer. In the following, Ω, Ω', and Ω'' will be chosen according to the QCTO guidelines presented in [7].

III. Numerical Results

To assess the features and the potentialities of the generalized QCTO methodology presented in Section II, let us consider, as a representative example, the synthesis of an *edge-shaped* array coated with a metamaterial lens [Fig. 1(*c*)] able to generate, outside the lens support, the same field distribution of a circular layout radiating in the free space [Fig. 1(*a*)].

With reference to the $2D$ scenario (i.e., $\bar{\bar{\varepsilon}}(\mathbf{r})$ and $\bar{\bar{\mu}}(\mathbf{r})$ are independent from z) where the *virtual* array [Fig. 1(*a*)] is an arrangement of $N = 20$ line sources located at $x_n = (\rho + \Delta\rho)\sin((d/\rho)(n-(N+1/2)))$, $y_n = (\rho+\Delta\rho)\cos((d/\rho)(n-(N+1/2)))$, $n = 1, \ldots, N$, with amplitudes

$$J_n = \exp\left(\frac{j2\pi\,(\rho+\Delta\rho)\cos\left(\frac{d}{\rho}\left(n-\frac{N+1}{2}\right)-\phi_s\right)}{\lambda}\right) \quad n = 1, \ldots, N \tag{14}$$

ϕ_s being the steering angle, $\Delta\rho = 0.25\lambda$ is the separation between the ground-plane and the antennas, $\rho = 5\lambda$ is the ground-plane radius, and $d = (\lambda/2)$ is the inter-element distance [Fig. 1(*a*)]. Under such an assumption, no geometrical transformation along z between the *virtual* and the *physical* geometry is needed and the deformation fields do not depend on z (i.e., $\mathbf{\Phi}(\mathbf{r}) = \mathbf{\Phi}(x, y)$ and $\mathbf{\Psi}(\mathbf{r}') = \mathbf{\Psi}(x', y')$). Moreover, the z-component of the deformation field is always unitary (i.e., $\Phi_z(\mathbf{r}) = z$ and $\Psi_z(\mathbf{r}') = z'$). By computing $\mathcal{J}[\mathbf{\Phi}(\mathbf{r})]$ and $\mathcal{J}[\mathbf{\Psi}(\mathbf{r}')]$ according to (10) and substituting in (13), it follows that

$$\varepsilon''_{xz}(\mathbf{r}'') = \varepsilon''_{yz}(\mathbf{r}'') = \varepsilon''_{zx}(\mathbf{r}'') = \varepsilon''_{zy}(\mathbf{r}'') = 0 \tag{15}$$

analogously to other state-of-the-art QCTO $2D$ problems [7]. The same holds true for the $\bar{\bar{\mu}}''(\mathbf{r}'')$ components.

In order to apply the generalized QCTO technique, the following geometries are defined:

- Ω (*virtual* geometry) [Fig. 1(*b*)]: circularly-eroded lens with $w = 16\lambda$, $t = 8\lambda$, $d = (\lambda/2)$, with dielectric properties $\bar{\bar{\varepsilon}}(\mathbf{r}) = \varepsilon_0 I$, $\bar{\bar{\mu}}(\mathbf{r}) = \mu_0 I$, I being the identity matrix;
- Ω' (*intermediate* geometry) [Fig. 1(*b*)]: rectangularly shaped lens with $w' = 16\lambda$ and $t' = 5\lambda$;

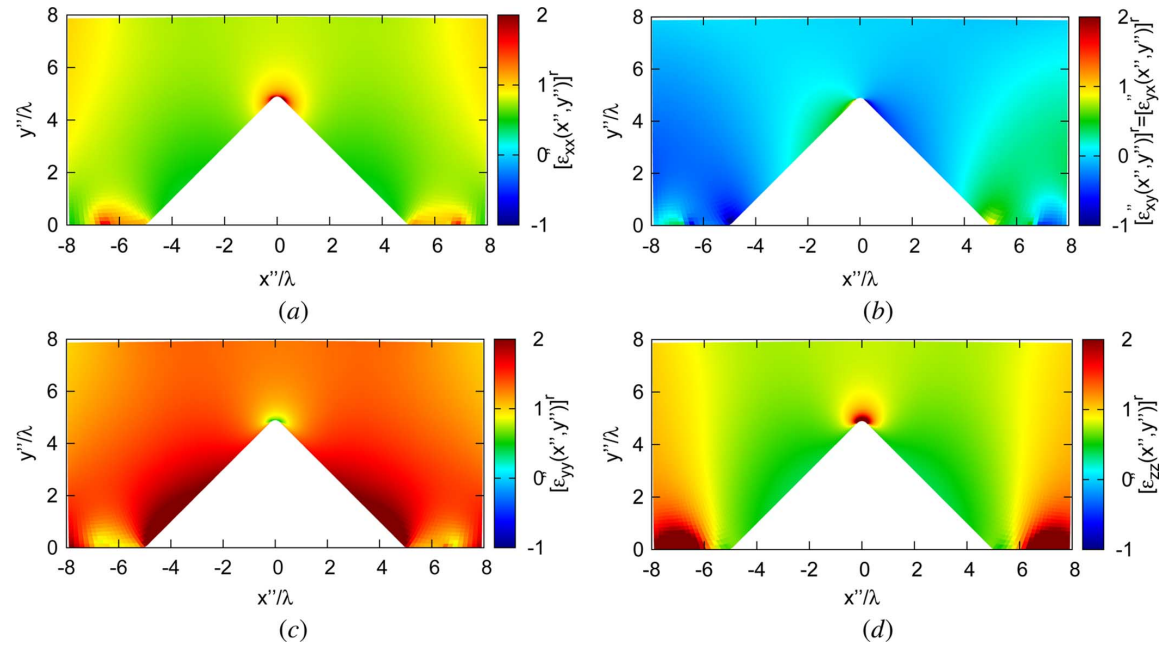

Fig. 2. [*Lens Design*] Relative permittivity distribution (normalized values) of the lens layout: (*a*) $[\varepsilon''_{xx}(\mathbf{r}'')]^r$, (*b*) $[\varepsilon''_{xy}(\mathbf{r}'')]^r = [\varepsilon''_{yx}(\mathbf{r}'')]^r$, (*c*) $[\varepsilon''_{yy}(\mathbf{r}'')]^r$, and (*d*) $[\varepsilon''_{zz}(\mathbf{r}'')]^r$.

- Ω'' (*physical* geometry) [Fig. 1(*c*)]: edge-eroded lens with $w'' = 16\lambda$, $t'' = 8\lambda$, $h'' = 5\lambda$, and $l'' = 10\lambda$.

The two-step QCTO approach is then carried out by first computing the deformation fields $\mathbf{\Phi}(x, y)$ and $\mathbf{\Psi}(x', y')$ by numerically solving (6) and (7). Towards this end, the technique in [18] is applied by discretizing Ω' with square cells of sides $(\lambda/50)$ and deducing the "deformed" grids in Ω and Ω'' that satisfy the Laplace's equation (Fig. 1). For the sake of clarity, the deformations computed in the two QCTO steps are pictorially represented with the grey dashed grids in Fig. 1(*a*)–(*c*). More specifically, the deformed geometry of the intermediate space is shown in Fig. 1(*b*) by assuming a coarse Cartesian grid with cells of side dimensions $\approx 0.7\lambda$.

By substituting the numerically-computed functions $\mathbf{\Phi}(x, y)$ and $\mathbf{\Psi}(x', y')$ in (13), the relative permittivity $[\bar{\bar{\varepsilon}}''(\mathbf{r}'')]^r \triangleq (\bar{\bar{\varepsilon}}''(\mathbf{r}'')/\varepsilon_0)$ (Fig. 2) is then obtained (the corresponding $\bar{\bar{\mu}}''(\mathbf{r}'')$ plots are not reported since, for symmetry reasons, they exactly correspond to those of the dielectric permittivity). As it can be noticed, the diagonal elements of the relative permittivity tensor [i.e., $[\varepsilon''_{xx}(\mathbf{r}'')]^r$—Fig. 2(*a*), $[\varepsilon''_{yy}(\mathbf{r}'')]^r$—Fig. 2(*c*), and $[\varepsilon''_{zz}(\mathbf{r}'')]^r$ - Fig. 2(*d*)] exhibit a range of variation between 1.0 and 2.0, with a concentration of the values significantly different from unity around the sharp edges of the lens. Such a result is actually expected from QCTO theory [7] because of the discontinuity in the slope of the ground-plane that causes higher values in the Jacobian of the deformation fields $\mathbf{\Phi}(\mathbf{r})$ and $\mathbf{\Psi}(\mathbf{r}')$ close to such regions. On the contrary, off-diagonal components of the permittivity tensor [i.e., $[\varepsilon''_{xy}(\mathbf{r}'')]^r$ and $[\varepsilon''_{yx}(\mathbf{r}'')]^r$—Fig. 2(*b*)] take values close to 0 almost everywhere [Fig. 2(*b*)], although they are negative in some regions [e.g., left portion of Fig. 2(*b*)], thus indicating an almost uniaxial anisotropy of the lens. Moreover, the permittivity profiles of the diagonal elements [i.e., $[\varepsilon''_{xx}(\mathbf{r}'')]^r$—Fig. 2(*a*) and $[\varepsilon''_{yy}(\mathbf{r}'')]^r$ - Fig. 2(*c*)] indicate a non-negligible medium anisotropy [e.g., Fig. 2(*a*) vs. Fig. 2(*c*)]. Such results point out that an isotropic lens is not generally sufficient to guarantee a suitable transformation when arbitrary conformal *virtual* and *physical* arrangements are under consideration (Fig. 1), unlike when one of the two geometries is linear [7]. Moreover, since $[\bar{\bar{\varepsilon}}''(\mathbf{r}'')]^r = [\bar{\bar{\mu}}''(\mathbf{r}'')]^r$ (see Section II), exactly the same conclusions can be drawn also concerning the associated permeability tensors.

For a consistency/validation check, the electromagnetic behavior of both the *physical* layout [Fig. 1(*c*)] and the *virtual* one [Fig. 1(*a*)] has been numerically simulated with a full-wave electromagnetic solver. The commercial software *COMSOL Multiphysics* has been used by enforcing $2D$ TM conditions[2]. The plots of $|E_z(\mathbf{r})|$ [Fig. 3(*a*)] and $|E''_z(\mathbf{r}'')|$ [Fig. 3(*b*)] (near field region) obtained for a steering angle equal to $\phi_s = 60$ [deg] assess the extremely good agreement between the field radiated by the circular arrangement in free space [Fig. 3(*a*)] and that generated by the edge-shaped arrangement coated with the QCTO lens [Fig. 3(*b*)]. This confirms the effectiveness and the reliability of the proposed two-step synthesis method. Such an outcome is further supported by the plots of the magnitude of the "difference field" [Fig. 3(*c*)] defined as

$$\Delta E_z(\mathbf{r}) \triangleq E_z(\mathbf{r}) - E''_z(\mathbf{r}'')|_{\mathbf{r}''=\mathbf{r}} \quad \mathbf{r} \notin \Omega \tag{16}$$

which is nearly negligible everywhere throughout the area outside the lens support [Fig. 3(*c*) vs. Fig. 3(*a*)]. As a matter of fact, the *virtual* and the *physical* configurations present the same radiation features with only minor differences [Fig. 3(*c*)] caused by the unavoidable discretization errors of the numerical solver.

The effectiveness of the QCTO-synthesized lens is even more evident when comparing it with a free-space edge-shaped array with the same geometry ("No Lens" configuration—Fig. 4). In this latter case, the difference field is of the same order of magnitude as $E_z(\mathbf{r})$ [Fig. 4(*b*) vs. Fig. 3(*a*)]. Analogously, a

[2]Under these assumptions, only the z-component of the electric field has to be computed.

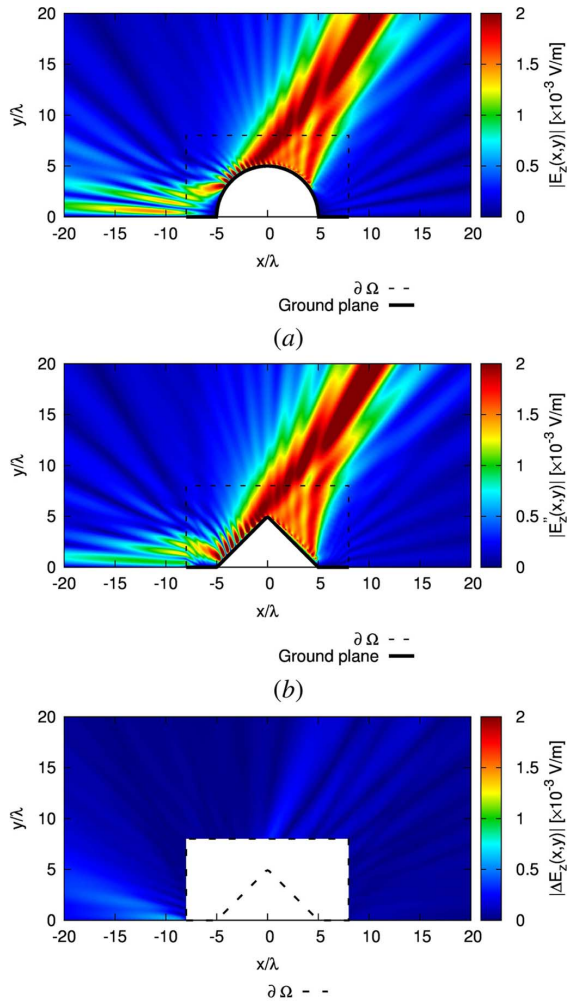

Fig. 3. [*Lens Performance*] Plots of (*a*) $|E_z(\mathbf{r})|$ and (*b*) $|E''_z(\mathbf{r}'')|$, and (*c*) difference field $|\Delta[E_z(\mathbf{r})]|$.

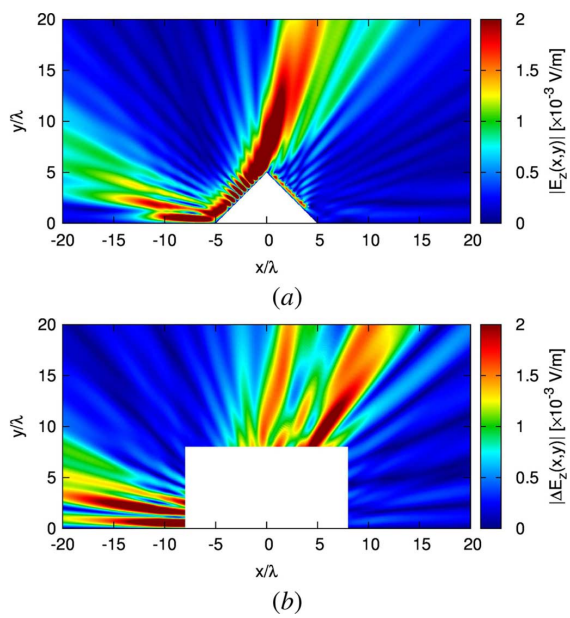

Fig. 4. [*Comparative Analysis*] Plots of (*a*) $|E_z(\mathbf{r})|$ and (*b*) difference field $|\Delta[E_z(\mathbf{r})]|$ for the "No Lens" configuration.

lens obtained by setting the off-diagonal elements of the permittivity and permeability tensors to zero would not be sufficient to guarantee satisfactory performance ("Uniaxial" configuration—Fig. 5). Indeed, the field difference in this test case [Fig. 5(*b*)] turns out comparable to the "No Lens" configuration [Fig. 4(*b*)]. Such a result suggests that the anisotropic nature of the synthesized lens is mandatory to achieve a suitable field control, unlike in simpler array design cases [7].

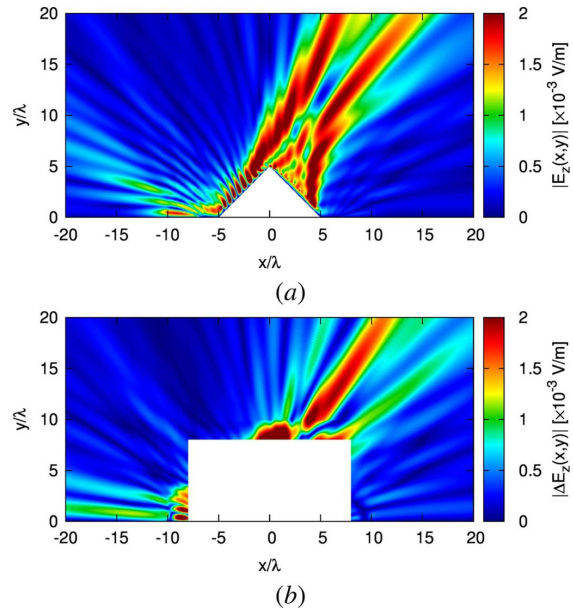

Fig. 5. [*Comparative Analysis*] Plots of (*a*) $|E_z(\mathbf{r})|$ and (*b*) difference field $|\Delta[E_z(\mathbf{r})]|$ for the "Uniaxial" configuration.

Similar considerations arise from the comparisons of the plots of the (far-field) normalized power pattern of the *virtual* and the *physical* layouts for different steering angles [$\phi_s = \{45, 90, 135\}$—Fig. 6(*a*)].[3] The matching between the pattern of the *physical* array and that of the *virtual* one turns out to be accurate whatever the steering angle [Fig. 6(*a*)] as also confirmed by the plot of the half-power beamwidth (HPBW) versus ϕ_s. As a matter of fact, $\mathrm{HPBW}(\phi_s)|_{\mathrm{virtual}} \approx \mathrm{HPBW}(\phi_s)|_{\mathrm{QCTO}}$ [Fig. 6(*b*)] for any $\phi_s \in [30, 150]$ [deg]. On the contrary, the beamwidth of the "No Lens" edge configuration significantly differs when varying the steering angle [Fig. 6(*b*)] as also expected from the near field results (Fig. 4). Moreover, the "Uniaxial" lens exhibits a HPBW similar to the *virtual* one when $\phi_s \approx 90$ [deg], while it can significantly differ for $\phi_s < 60$ [deg] or $\phi_s > 120$ [deg] [Fig. 6(*b*)], as it was predicted by the plots in Fig. 5.

As for the computational issues of the proposed synthesis method, the lens synthesis (i.e., the Laplace's problem and the Jacobian computation for the two steps) required about 6.2×10^2 [s] on a standard laptop running at 2.40 GHz when using a non-optimized Matlab implementation, while the full-wave simulation took about 2.4×10^3 [s] for each steering angle. This suggests that an Evolutionary Optimization loop aimed at refining the shape of Ω, Ω', and Ω'' to enhance the lens features (e.g., to reduce the lens medium anisotropy) is not currently feasible from the numerical viewpoint because of the need to synthesize and simulate the lens (i.e., the computation of the cost function measuring the mismatch between *virtual* and *physical*

[3]The far field patterns have been numerically computed with COMSOL by using the *Stratton-Chu* formula [21].

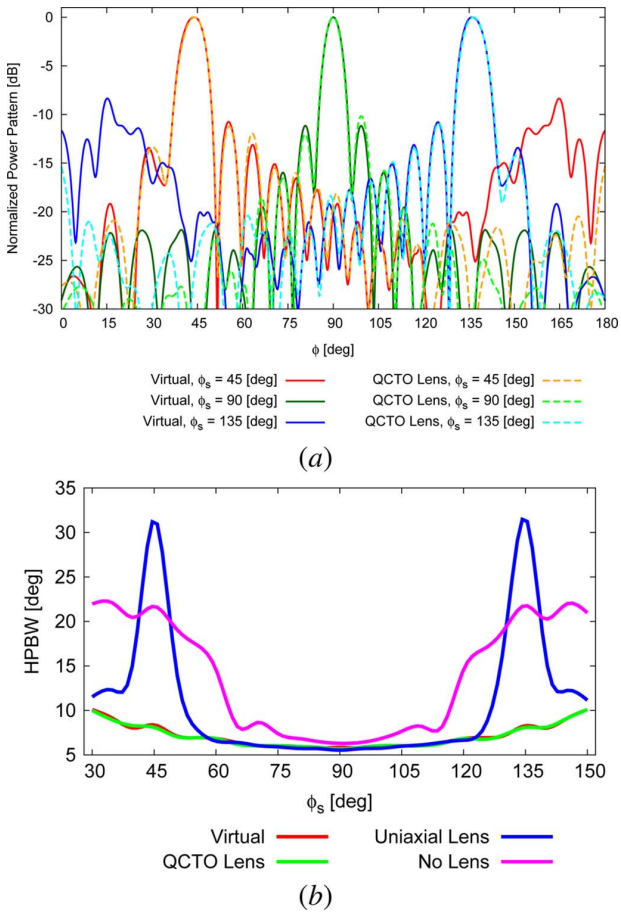

Fig. 6. [*Comparative Analysis*] (*a*) Directivity patterns for the configurations in Fig. 1(*a*) and (*c*) when $\phi_s = \{45, 90, 135\}$ [deg]. (*b*) Plot of the FNBW as a function of the steering angle for the "Virtual", "QCTO Lens", "Uniaxial", and "No Lens" configurations.

electromagnetic behavior) several times to reach convergence [19], [20]. This issue could be overcome, however, by creating *ad-hoc* tools devoted to increasing the speed of the functional evaluation within the *Material-by-Design* loop.

IV. Conclusions and Remarks

In this work, a transformation optics methodology has been proposed to design inhomogeneous metamaterial lenses able to control the radiation properties of arbitrary-shaped antenna arrays (*physical* arrangements) so that they exhibit the same radiating features of arbitrary *virtual* arrays.

From the methodological viewpoint, the main contribution of this work is the generalization of the QCTO technique presented in [7] to effectively deal with arbitrary *virtual* and *physical* layouts while yielding almost uniaxial lens parameters. Towards this end, the solution of two connected Laplace's problems has been carried out to deduce the overall deformation field and, successively, TO rules have been exploited to compute the lens dielectric parameters. Such a two-step QCTO methodology has been assessed for the case of a $2D$ array synthesis problem related to an edge-conformal layout comprising $N = 20$ antennas and matching the radiation of a *virtual* circular arrangement. Full-wave numerical simulations have verified the reliability of the two-step QCTO method in controlling the radiation features of conformal arrangements regardless of the steering angle.

Further investigations, beyond the scope of the present paper, will be devoted to the extension of the two-step QCTO method to $3D$ structures, as well as to its integration within Evolutionary Optimization loops [19], [20]. This would allow the designer to further simplify the dielectric features of the lenses by targeting realistic/available materials while at the same time enhancing their performance. As for this latter research item, the choice of the shape and dimensions of the domains Ω, Ω', and Ω'' will be a key-challenge to be addressed since it strongly affects the performance of the synthesized devices as well as its impact on their practical feasibility. Furthermore, additional studies aimed at addressing the potential difficulties in the realization of the two-step QCTO designs (caused by the arbitrary gradients in the permittivity and permeability tensors) are envisaged. Toward this end, the generalization of state-of-the-art processes for the fabrication of TO lenses [22] to the layouts of interest is currently under investigation.

References

[1] J. Boyns, C. Gorham, A. Munger, J. Provencher, J. Reindel, and B. I. Small, "Step-scanned circular-array antenna," *IEEE Trans. Antennas Propag.*, vol. 18, no. 5, pp. 590–595, Sep. 1970.

[2] K. Alkhalifeh, R. Sarkis, and C. Craeye, "Design of a novel 3D circular Vivaldi antennas array for ultra-wideband near-field radar imaging," in *Proc. Eur. Conf. on Antennas Propag.*, Mar. 26–30, 2012, pp. 898–901.

[3] J.-A. Tsai, R. Buehrer, and B. D. Woerner, "BER performance of a uniform circular array versus a uniform linear array in a mobile radio environment," *IEEE Trans. Wireless Comm.*, vol. 3, no. 3, pp. 695–700, May 2004.

[4] N. J. G. Fonseca, "Design and implementation of a closed cylindrical BFN-fed circular array antenna for multiple-beam coverage in azimuth," *IEEE Trans. Antennas Propag.*, vol. 60, no. 2, pp. 863–869, Feb. 2012.

[5] G. A. Thiele and C. Donn, "Design of a small conformal array," *IEEE Trans. Antennas Propag.*, vol. 22, no. 1, pp. 64–70, Jan. 1974.

[6] Y. Luo, J. Zhang, L. Ran, H. Chen, and J. A. Kong, "New concept conformal antennas utilizing metamaterial and transformation optics," *IEEE Antennas Wireless Propag. Lett.*, vol. 7, pp. 509–512, Jul. 2008.

[7] D.-H. Kwon, "Quasi-conformal transformation optics lenses for conformal arrays," *IEEE Antennas Wireless Propag. Lett.*, vol. 11, pp. 1125–1128, Sep. 2012.

[8] Y. Lee and Y. Hao, "Figure-of-merit analysis of resonant particles for construction of practical metamaterials," *IEEE Antennas Wireless Propag. Lett.*, vol. 7, pp. 167–170, 2008.

[9] A. Massa, G. Oliveri, P. Rocca, and F. Viani, "System-by-design: A new paradigm for handling design complexity," in *Proc. Eur. Conf. on Antennas Propag.*, Apr. 6–11, 2014, pp. 1423–1426.

[10] H. Chen, C. T. Chan, and P. Sheng, "Transformation optics and metamaterials," *Nature Mater.*, vol. 9, pp. 387–396, May 2010.

[11] D.-H. Kwon and D. H. Werner, "Transformation electromagnetics: An overview of the theory and applications," *IEEE Antennas Propag. Mag.*, vol. 52, no. 1, pp. 24–46, Feb. 2010.

[12] , D. H. Werner and D.-H. Kwon, Eds., *Transformation Electromagnetics and Metamaterials: Fundamental Principles, and Applications*. London, U.K.: Springer, 2014.

[13] W. Tang, C. Argyropoulos, E. Kallos, W. Song, and Y. Hao, "Discrete coordinate transformation for designing all-dielectric flat antennas," *IEEE Trans. Antennas Propag.*, vol. 58, no. 12, pp. 3795–3804, Dec. 2010.

[14] D. Bao, R. C. Mitchell-Thomas, K. Z. Rajab, and Y. Hao, "Quantitative study of two experimental demonstrations of a carpet cloak," *IEEE Antennas Wireless Propag. Lett.*, vol. 12, pp. 206–209, 2013.

[15] Z. Chang, X. Zhou, J. Hu, and G. Hu, "Design method for quasi-isotropic transformation materials based on inverse Laplace's equation with sliding boundaries," *Opt. Expr.*, vol. 18, pp. 6089–6096, 2010.

[16] J. Hu, X. Zhou, and G. Hu, "Design method for electromagnetic cloak with arbitrary shapes based on Laplace's equation," *Opt. Expr.*, vol. 17, pp. 1308–1320, 2009.

[17] J. B. Pendry, D. Schurig, and D. R. Smith, "Controlling electromagnetic fields," *Science*, vol. 312, pp. 1780–1782, Jun. 2006.

[18] D. C. Ives and R. M. Zacharias, "Conformal mapping and orthogonal grid generation," presented at the AIAA/SAE/ASME/ASEE 23rd Joint Propulsion Conf., San Diego, CA, USA, Jun. 1989, paper no. 87-2057.

[19] P. Rocca, M. Benedetti, M. Donelli, D. Franceschini, and A. Massa, "Evolutionary optimization as applied to inverse scattering problems," *Inv. Probl.*, vol. 25, no. 12, pp. 1–41, Dec. 2009.
[20] P. Rocca, G. Oliveri, and A. Massa, "Differential evolution as applied to electromagnetics," *IEEE Antennas Propag. Mag.*, vol. 53, no. 1, pp. 38–49, Feb. 2011.
[21] J. A. Stratton and L. J. Chu, "Diffraction theory of electromagnetic waves," *Phys. Rev.*, vol. 56, pp. 99–107, 1939.
[22] C. Mateo-Segura, A. Dyke, H. Dyke, S. Haq, and Y. Hao, "Flat Luneburg lens via transformation optics for directive antenna applications," *IEEE Trans. Antennas Propag.*, vol. 62, no. 4, pp. 1945–1953, Apr. 2014.

Giacomo Oliveri (M'07–SM'13) received the B.S. and M.S. degrees in telecommunications engineering and the Ph.D. degree in space sciences and engineering from the University of Genoa, Italy, in 2003, 2005, and 2009 respectively.

He is currently an Assistant Professor at the Department of Information Engineering and Computer Science (University of Trento) and a member of the ELEDIA Research Center. He was a Visiting Researcher at the Laboratoire des signaux et systèmes (L2S)@Supélec, Paris, France, in 2012 and 2013. Since 2014, he has been an Invited Associate Professor at the University of Paris Sud, Paris, France. He is an author/coauthor of over 200 peer reviewed papers on international journals and conferences. His research work is mainly focused on electromagnetic direct and inverse problems, system-by-design and metamaterials, and antenna array synthesis.

Dr. Oliveri serves as an Associate Editor of the *International Journal of Distributed Sensor Networks* and of the *Microwave Processing Journal*.

Ephrem T. Bekele received the B.Sc. degree in electrical engineering from Bahir Dar University, Bahir Dar, Ethiopia, in 2007 and the M.Sc. degree in telecommunications engineering from the University of Trento, Trento, Italy, in 2011.

He worked as an Assistant Lecturer in Bahir Dar University, from 2007 to 2009. He is currently a Ph.D. student at the ICT International Doctoral School of Trento, and conducting research in the ELEDIA Research Center. His main research interests are antenna arrays and electromagnetic inverse scattering.

Douglas H. Werner (F'05) received the B.S., M.S., and Ph.D. degrees in electrical engineering and the M.A. degree in mathematics from the Pennsylvania State University (Penn State), University Park, PA, USA, in 1983, 1985, 1989, and 1986, respectively.

He is the John L. and Genevieve H. McCain Chair Professor in the Pennsylvania State University Department of Electrical Engineering. He is also the Director of the Computational Electromagnetics and Antennas Research Lab (CEARL: http:// cearl.ee.psu.edu/) as well as a member of the Communications and Space Sciences Lab (CSSL). He is also a faculty member of the Materials Research Institute (MRI) at Penn State. His research interests include computational electromagnetic, antenna theory and design, phased arrays (including ultra-wideband arrays), microwave devices, wireless and personal communication systems (including on-body networks), wearable and e-textile antennas, RFID tag antennas, conformal antennas, reconfigurable antennas, frequency selective surfaces, electromagnetic wave interactions with complex media, metamaterials, electromagnetic bandgap materials, zero and negative index materials, transformation optics, nanoscale electromagnetics (including nanoantennas), fractal and knot electrodynamics, and nature-inspired optimization techniques (genetic algorithms, clonal selection algorithms, particle swarm, wind driven optimization, and various other evolutionary programming schemes). He holds seven patents, has published over 575 technical papers and proceedings articles, and is the author of 12 book chapters with two additional chapters currently in preparation. He has published several books including *Frontiers in Electromagnetics* (Piscataway, NJ: IEEE Press, 2000), *Genetic Algorithms in Electromagnetics* (Hoboken, NJ: Wiley/IEEE, 2007), and *Transformation Electromagnetics and Metamaterials: Fundamental Principles and Applications* (London, UK: Springer, 2014). He has also contributed chapters for several books including *Electromagnetic Optimization by Genetic Algorithms* (New York: Wiley Interscience, 1999), *Soft Computing in Communications* (New York: Springer, 2004), *Antenna Engineering Handbook* (New York: McGraw-Hill, 2007), *Frontiers in Antennas: Next Generation Design and Engineering* (New York: McGraw-Hill, 2011), *Numerical Methods for Metamaterial Design* (New York: Springer, 2013), and *Computational Electromagnetics* (New York: Springer, 2014).

Dr. Werner is a member of the American Geophysical Union (AGU), URSI Commissions B and G, the Applied Computational Electromagnetics Society (ACES), Eta Kappa Nu, Tau Beta Pi and Sigma Xi. He is a Fellow of the IEEE, the IET (formerly IEE), and ACES. He was presented with the 1993 Applied Computational Electromagnetics Society (ACES) Best Paper Award and was also the recipient of a 1993 International Union of Radio Science (URSI) Young Scientist Award. In 1994, he received the Pennsylvania State University Applied Research Laboratory Outstanding Publication Award. He was a coauthor (with one of his graduate students) of a paper published in the IEEE TRANSACTIONS ON ANTENNAS AND PROPAGATION which received the 2006 R. W. P. King Award. He received the inaugural IEEE Antennas and Propagation Society Edward E. Altshuler Prize Paper Award and the Harold A. Wheeler Applications Prize Paper Award in 2011 and 2014 respectively. He has also received several Letters of Commendation from the Pennsylvania State University Department of Electrical Engineering for outstanding teaching and research. He is a former Associate Editor of *Radio Science*, an Editor of the *IEEE Antennas and Propagation Magazine*. He was the recipient of a College of Engineering PSES Outstanding Research Award and Outstanding Teaching Award in March 2000 and March 2002, respectively. He was also presented with an IEEE Central Pennsylvania Section Millennium Medal. In March 2009, he received the PSES Premier Research Award.

Jeremiah P. Turpin (M'13) received the B.S. degree in electrical engineering from Grove City College, Grove City, PA, USA, in 2009 and the M.S. degree in electrical engineering from the Pennsylvania State University, University Park, PA, USA, in 2011.

He is currently a Graduate Research Assistant in the Computational Electromagnetics and Antennas Research Laboratory, Department of Electrical Engineering, The Pennsylvania State University, where he has been investigating transformation optics designs for antenna applications and developing metamaterials for implementation of TO devices. His other research experience includes the investigation of metamaterials for optical and near-infrared systems, reconfigurable radio-frequency metamaterials, and optical ray tracer development.

Andrea Massa (M'03) received the "Laurea" degree in electronic engineering from the University of Genoa, Genoa, Italy, in 1992 and Ph.D. degree in electronics and computer science from the same university in 1996.

From 1997 to 1999, he was an Assistant Professor of electromagnetic fields at the Department of Biophysical and Electronic Engineering, University of Genoa, teaching the university course of electromagnetic fields 1. From 2001 to 2004, he was an Associate Professor at the University of Trento. Since 2005, he has been a Full Professor of Electromagnetic Fields at the University of Trento, where he currently teaches electromagnetic fields, inverse scattering techniques, antennas and wireless communications, and optimization techniques.

At present, he is the Director of the ELEDIA Research Center, University of Trento. In addition, he is an Adjunct Professor at the Pennsylvania State University (Penn State), University Park, PA, USA, and a Visiting Professor at the Missouri University of Science and Technology, Rolla, MO, USA, at Nagasaki University, Japan, at the University of Paris Sud, France, and at Kumamoto University, Kumamoto, Japan. Since 1992, his research work has been principally focused on electromagnetic direct and inverse scattering, microwave imaging, optimization techniques, wave propagation in presence of nonlinear media, wireless communications and applications of electromagnetic fields to telecommunications, medicine and biology.

Prof. Massa is a member of the IEEE Society, of the PIERS Technical Committee, and of the Inter-University Research Center for Interactions Between Electromagnetic Fields and Biological Systems (ICEmB). He has served as Italian representative in the general assembly of the European Microwave Association (EuMA). He serves as an Associate Editor of the IEEE TRANSACTIONS ON ANTENNAS AND PROPAGATION.